Jurnal Kejuruteraan 37(3) 2025: 1069-1083
https://doi.org/10.17576/jkukm-2025-37(3)-01

Acoustic Emission Characteristics of Real-time Monitoring on Asphalt Pavement

Khairul Afinawati Hashim[a*], Noorsuhada Md Nor[a], Shahrum Abdullah[b] & Nurul Khirna Fazlina Khir Johari[a]

[a]*Centre for Civil Engineering Studies Programme,*
Universiti Teknologi MARA, Cawangan Pulau Pinang, Malaysia

[b]*Department of Mechanical and Manufacturing Engineering,*
Faculty of Engineering & Built Environment, Universiti Kebangsaan Malaysia, Malaysia

[*]*Corresponding author: khairul_afinawati@uitm.edu.my*

Received 14 August 2024, Received in revised form 26 December 2024
Accepted 26 June 2025, Available online 30 May 2025

ABSTRACT

This paper presents the acoustic emission characteristics for asphalt pavements under real load conditions. With the increasing number of vehicles on the roadways causing more damage and deterioration to asphalt pavements, effective monitoring is necessary to prolong the life of asphalt pavement structures. To determine these properties, real-time monitoring of asphalt pavements using acoustic emissions technique was conducted in the field. The study focused on Lebuh Ilmu Road at Universiti Kebangsaan Malaysia, a continuation of the main federal road. This real-time monitoring was carried out from 8:00 am to 9:30 am, and the number of passing vehicles was counted. Three sensors were placed on the roadway at 2 m intervals using magnetic holders. The acoustic emission data collected by the sensors were digitized, stored, and visualized. The parameters of the acoustic emissions including amplitude, rise time, rise angle, and average frequency were analyzed and discussed. The study revealed that there was a difference in the variation of the acoustic emission parameters, influenced by the cyclic loading of passing vehicles. The values of the acoustic emission parameters such as amplitude, rise time, rise angle, and average frequency increased with the increasing cyclic loading by passing vehicles. This suggests that the application of acoustic emissions in asphalt pavements has great potential for determining the integrity of the pavement structure.

Keywords: Asphalt pavement; acoustic emission; real-time monitoring; cyclic loading; average frequency

INTRODUCTION

Asphalt pavements experience deterioration over time due to various factors, including traffic loading, climatic conditions, and aging. Currently, various damage detection techniques, such as image measurement, computed tomography (CT), and the falling weight deflectometer (FWD), are extensively utilized for crack monitoring and performance evaluation of asphalt pavements (Qiu et al. 2020). Although effective in diagnosing and visualizing pavement distresses, these methods are limited in the capacity to continuously monitor the complete process of pavement damage in real time. As noted by Cong et al. (2016) and Wei et al. (2023), different traffic types exert varying loading values and mechanical stresses on asphalt pavement over time, influencing the material's deformation. Furthermore, existing methods are mostly limited to surface-level detection and are inadequate for monitoring internal crack development within asphalt pavement structures. To address these limitations, methods capable of assessing pavement quality non-destructively while also facilitating the monitoring of internal crack progression within the asphalt pavement structure are needed.

Therefore, the acoustic emission (AE) technique is a non-destructive method that offers several features, such as real-time and comprehensive detection (Shen et al. 2015; Md Nor et al. 2016). This method occurs when energy is rapidly released from a localized source or sources within a material, resulting in transient elastic waves (Shen et al. 2015). According to Li and Marasteanu (2006), AE is a transient elastic wave caused by the release of energy from

localized damage processes within a stressed material. As a result of this energy release, stress waves are scattered and can be detected at the material's surface. Due to its capability, the AE method has been extensively used for engineering materials and structural health monitoring (SHM). It has been employed to investigate the behaviour of various materials such as concrete and rock (Md Nor et al. 2021; Hashim et al. 2021), as well as steel, and to assess the performance of numerous types of concrete and road surfaces.

Wei et al. (2023) conducted a study on the effect of loading rate on failure characteristics of asphalt mixtures using AE technique. Qiu et al. (2022) utilized AE to exploring characteristics and behaviors of mixed-mode fracture process of asphalt mixtures. Apeagyei et al. (2009); Apeagyei (2013) investigated the brittleness of asphalt binders at low temperatures and the stability of foamed asphalt using AE. Hill et al. (2013) examined AE activities in warm mixed asphalt during rapid temperature drops. Additionally, Arnold et al. (2014) employed the AE approach to determine the embrittlement temperatures of a combination of recycled asphalt and shingles. Behnia et al. (2016) analysed the cracking behaviour of different asphalt materials as part of a recent study on low temperature cracking. Behnia et al. (2018) further investigated the cracking behaviour of asphalt pavements at low temperatures, which were assessed using the AE technique.

Previous studies have demonstrated the significant potential of the AE technique for damage assessment. However, most of these investigations have been conducted in controlled laboratory settings using asphalt mixture test specimens, with only a limited number of studies focusing on the real-time monitoring of asphalt pavements in the field. The aim of this study is to employ the AE technique for real-time monitoring and to investigate the variation characteristics of AE signals within asphalt pavement structures. The findings are expected to enhance the understanding of microcrack initiation in field conditions.

METHODOLOGY

In this section, the methodology for the study is described in detail. Figure 1 illustrates the process for determining the AE characteristics of asphalt pavements under real load conditions. The initial step involved identifying the problem with the current methods of asphalt pavement monitoring that are subjected to daily traffic from various vehicles. Next, a suitable road section frequently used for traffic was chosen. The method for real-time monitoring was then determined, and AE monitoring was employed in this study. All AE-related instruments were placed on the selected road section. To ensure a proper connection between the sensor surface and the asphalt surface, sensor verification was conducted using a pencil break technique. Additionally, a noise test was performed to establish the threshold. Once all necessary parameters were identified, the AE monitoring began, and the number of passing vehicles was recorded. Subsequently, the collected data were analyzed to determine the AE characteristics for asphalt pavement structures.

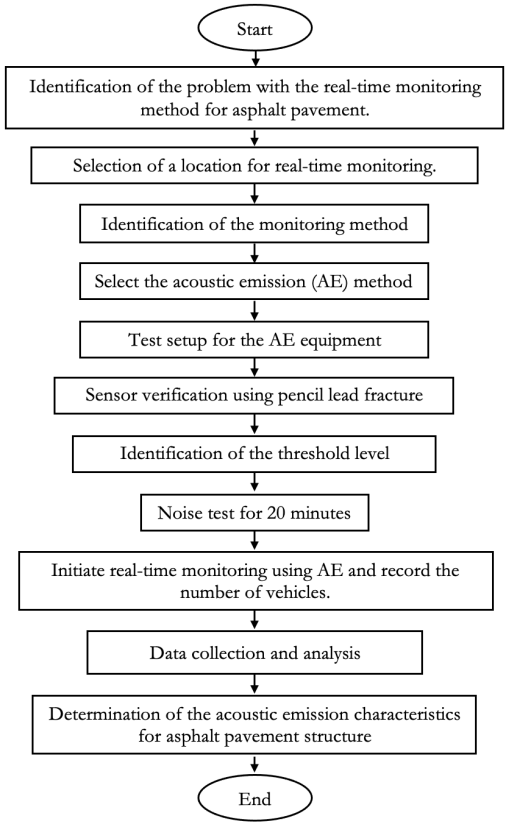

FIGURE 1. Flow process of real-time monitoring on asphalt pavement using AE

TEST SETUP

Lebuh Ilmu Road, located in Universiti Kebangsaan Malaysia (UKM) Bangi, Selangor, was selected as the designated field monitoring site for this study. This road is classified as an asphalt road with medium geometric features and a pavement width of 3.25 meters. The maximum speed allowed on this road is 70 km/h. The real-time AE monitoring setup is illustrated in Figures 2 and 3.

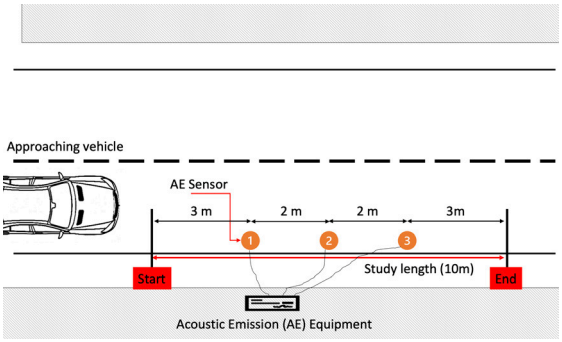

FIGURE 2. Schematic diagram of AE real-time monitoring test setup

The field monitoring test was conducted on a 10 m section, as shown in Figure 2. Three AE sensors were attached to the pavement surface using steel plates. The plates were bonded to the surface to secure the sensors, and magnetic holder legs were then attached to the plates. The sensors were placed in the magnetic holders. The intervals between the sensor clamping locations on the asphalt were 3 m, 2 m, 2 m, and 3 m. High vacuum grease was applied as a coupling agent between the asphalt surface and the bottom sensor. The test was conducted in the morning, starting at 8:00 am and ending at 9:30 am, to minimize any potential temperature-related effects on the sensors. Additionally, three cones were placed near the sensors to warn road users.

FIGURE 3. AE real-time monitoring test setup

ACOUSTIC EMISSION (AE) MONITORING

The AE was monitored using a multi-channel AMSY-5 system. This system comprises piezoelectric AE sensors (VS75-V) with a frequency range of 30-120 kHz, an external preamplifier, a two-channel signal processor (ASIP-2), magnetic holders, and a visual monitor equipped with comprehensive AE software for data acquisition and analysis. Three sensors were placed on the surface of the asphalt pavement using magnetic holders. The sensors must be securely attached to the road surface to ensure proper sensor utilization during testing. This mounting technique prevents sensor movement and minimizes transmission losses between the road surface and the sensor's sensitive surface. Additionally, a thin layer of high vacuum grease is applied as an adhesive to ensure consistent adhesion between the sensors and the road surface. To verify the

sensitivity of the sensors, a pencil lead fracture (PLF) test was performed. For this test, a magnetic pencil with a Teflon shoe (Nielsen shoe) was used to break a 0.5 mm 2H lead, thereby generating a simulated acoustic wave on the surface of the asphalt pavement. The procedure for handling the magnetic pencil was described in ASTM E976-15 (2015). It was considered that all sensors were effectively coupled if the wave generated by at least three or more repetitions of the PLF test resulted in a high amplitude of 99 dB or if the sensitivity varied within ±3 dB (Hashim et al. 2021; ASTM, 2015; Md Nor et al. 2013).

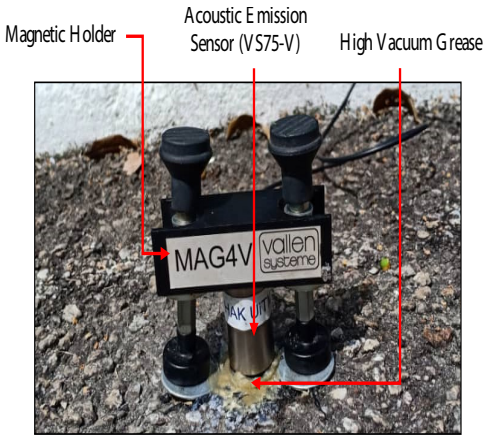

FIGURE 4. AE sensor, magnetic holder and couplant

The noise test was conducted to establish the optimal threshold value, which can be stored in the AE hardware and employed during the monitoring procedure. Initially, a low threshold of 20 dB was set in the noise test, and the AE system operated for approximately 20 minutes. Subsequently, the maximum amplitude within the time window was identified and suggested as the threshold for the AE hardware. Based on the noise test results, a threshold of 30 dB was set into the AE hardware. This threshold effectively eliminates noise interference during the acoustic monitoring of the asphalt pavement.

DATA COLLECTION FOR TRAFFIC VOLUME

Data collection for traffic volume count is a crucial aspect of the methodological process in this study. The purpose of this volume count was to evaluate the impact on traffic flow during real-time monitoring. Traffic volume data was gathered through the manual counting method using tally sheets. Furthermore, vehicles' classification and loading conditions were documented at 30-minute intervals. The vehicle classification employed in this study adhered to the guidelines provided by PLUS Malaysia Berhad, as presented in Table 1.

TABLE 1. Vehicle classes according to PLUS Malaysia Berhad

Class	Description
Class 1	Vehicle with 2 axles and 3- or 4-wheels excluding taxis
Class 2	Vehicle with 2 axles and 5- or 6-wheels excluding buses
Class 3	Vehicle with 3 or more axles
Class 4	Taxis
Class 5	Busses

DATA ANALYSIS

In this study, the variation patterns of the characteristic parameters of AE were extracted from real-time monitoring data. The analysis focused on the basic parameters of AE, namely amplitude, rise time, rise angle, and average frequency. Amplitude is the highest measured voltage in a waveform, expressed in decibels (dB). Rise time is the time interval between the first crossing of the threshold and the peak signal. Duration is the time difference between the first and last crossing of the threshold. Counts refer to the number of pulses generated by the measuring circuit when the signal amplitude exceeds the threshold. The average frequency is the ratio of counts to duration, while the rise angle value is the ratio of rise time to amplitude. The average frequency and rise angle equations are shown in equations (1) and (2), respectively.

Average frequency = Count/Duration (1)

Rise angle = Rise time/Amplitude (2)

All AE parameters, including rise time, amplitude, and rise angle versus time, were analyzed in the time domain. The analysis of each parameter is divided into three-time intervals, with the data analysis of these parameters also being divided accordingly. Each interval is 1800 seconds, equivalent to 30 minutes, as shown in Table 2. The relationship between the average frequency and the rise angle was also analyzed and discussed.

TABLE 2. Three intervals of time

Interval	Time, s	Duration
1st Interval	0-1800	8.00-8.30am
2nd Interval	1800-3600	8.30-9.00am
3rd Interval	3600-5400	9.00-9.30am

RESULTS AND DISCUSSION

TRAFFIC VOLUME COUNT

Traffic volume counts were conducted to assess the impact on traffic flow during real-time monitoring. The traffic volume data was obtained through manual counting on counting sheets. The classification and loading conditions of passing vehicles were recorded every 30 minutes. Table 3 presents the traffic volume count data. In this table, traffic volume was counted based on the weight of Class 1 and Class 2 vehicles, measured in kN. Class 1 vehicles refer to those with two axles, four wheels, and a weight of 30 kN per vehicle. Class 2 vehicles, on the other hand, include vehicles with 5 or 6 wheels (excluding buses) and a weight of 60 kN. Observations revealed that most Class 1 and 2 vehicles passed through this road, primarily serving students and university staff, during the 1st and 2nd intervals. However, only Class 1 vehicles were observed to pass through this road during the 3rd interval. Table 3 demonstrates that during the 1st interval, the lowest number of vehicles passed through the monitoring area, with only 52 vehicles recorded. In the 2nd interval, which corresponds to the morning hours between 8:30 am and 9:00 am, many vehicles (125 vehicles) utilized the road, primarily consisting of academic staff. During the 3rd interval, a total of 102 vehicles used this road. This number of vehicles affected the characteristics that impact the performance and integrity of the asphalt pavements, as this road is considered a major thoroughfare within the university. Since the AE monitoring was conducted, the characteristics of the asphalt pavement can be identified based on AE parameters, which will be discussed later. These AE characteristics can be utilized to assess the integrity of the asphalt pavement and are highly useful in predicting the road's performance.

TABLE 3. Traffic volume count data (Sources: Class of vehicle is referred from PLUS Malaysia Berhad)

		Average Weight of Vehicle, kN		Time Spotted on Road, s	
Interval	No. of Vehicles	Class 1	Class 2	Class 1	Class 2
1st Interval	52	30	60	0-1800	1500-1800
2nd Interval	125	30	60	1800-3600	2340-2400
3rd Interval	102	30	60	3600-5400	-

ACOUSTIC EMISSION (AE) AMPLITUDE

Figures 5, 7, and 9 depict the distribution of acoustic emission (AE) amplitude from three different channels at three intervals. For this analysis, the signals captured by sensors 1, 2, and 3 have been labelled as CH1, CH2, and CH3, respectively. The figures reveal that a significant number of amplitudes were observed in the range of 30 dB to 32 dB across all intervals.

Figures 6, 8, and 10 display the waveform of the signal with the highest amplitude for each interval. From these waveforms, the characteristics of the asphalt pavement can be discerned. Figure 5 demonstrates that CH2 recorded more instances of amplitude at the 1st interval compared to the other two channels. However, CH3 recorded the highest amplitude between 400 s and 600 s when vehicles passed over the road. Additionally, Figure 5 exhibits a substantial scattering of high amplitudes between 300 s and 600 s when a total of 20 Class 1 and 2 vehicles traversed the road and passed through the monitoring area. These vehicles significantly impacted the asphalt pavement, resulting in heightened AE activity. The highest amplitude within this interval was recorded as 53 dB at 530 s when the Class 2 vehicles passed over the road. Lower amplitudes were observed after 600 s, as most Class 1 vehicles had already passed. The majority of amplitudes was recorded after 600 s were below 35 dB.

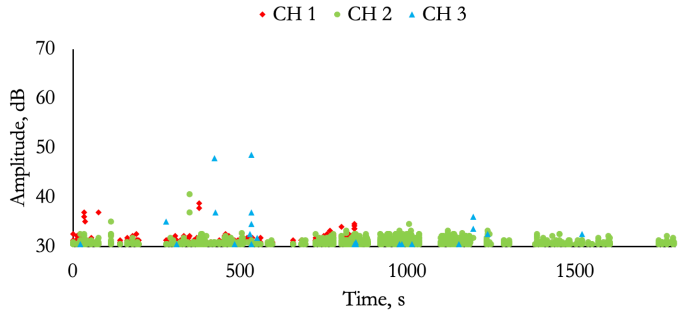

FIGURE 5. Amplitude against time at different channel for asphalt pavement (1st Interval)

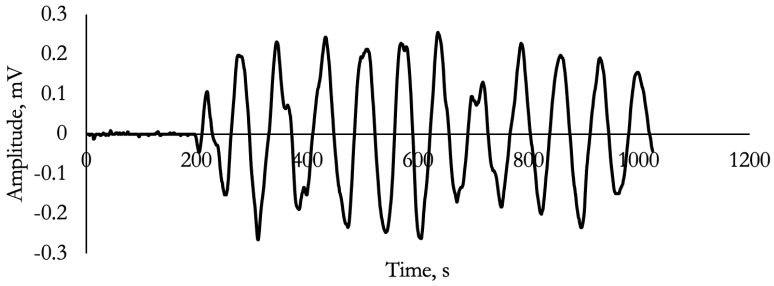

FIGURE 6. Maximum signal for peak amplitude at 1st interval

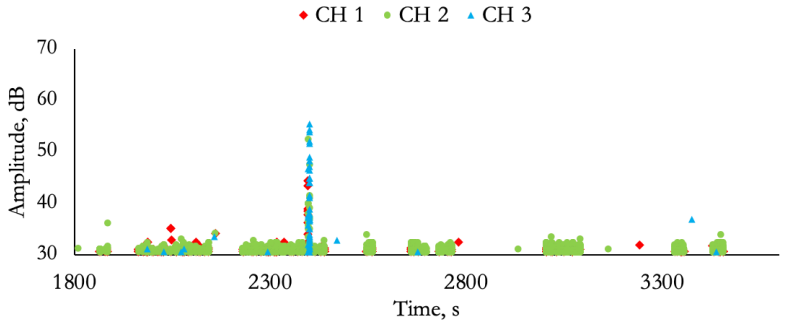

FIGURE 7. Amplitude against time at different channel for asphalt pavement (2nd Interval)

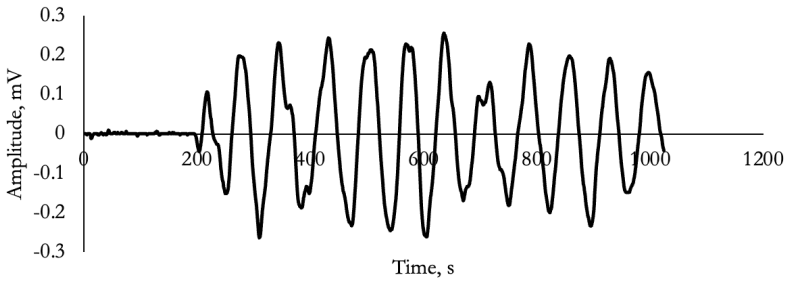

FIGURE 8. Maximum signal for peak amplitude at 2nd interval

For the 2nd interval, as shown in Figure 7, most of the AE amplitudes were recorded in the range of 34 dB for all sensors. A total of 152 Class 1 and Class 2 vehicles passed the road during the AE monitoring. The monitoring was conducted from 1800 s to 3600 s. A large number of Class 2 vehicles were recorded between 2340 s and 2400 s. This increased number of Class 2 vehicles resulted in a high amplitude of 58 dB observed at 2399 s. This high amplitude

produced a large negative waveform of 0.265 mV, as shown in Figure 8. Ma and Du (2017) found that the high amplitude was due to the high loading at a specific location. When the Class 2 vehicles, each weighing 60 kN, passed the road between 2340 s and 2400 s, they generated a significant load and impact on the asphalt.

In Figure 9, a large number of scattered AE events were identified based on the amplitudes. Most of the high amplitudes were recorded in CH1. The highest amplitude in this interval was 62.2 dB at time 5000 s. This highest amplitude produced a positive AE waveform of 1.25 mV, as shown in Figure 10. Although no Class 2 vehicles were observed in this interval, a significant number of Class 1 vehicles led to the formation of high amplitudes during specific time periods. This can be observed at Spot A and Spot B in the time range of 3700 s to 3900 s and 4900 s to 5200 s, respectively.

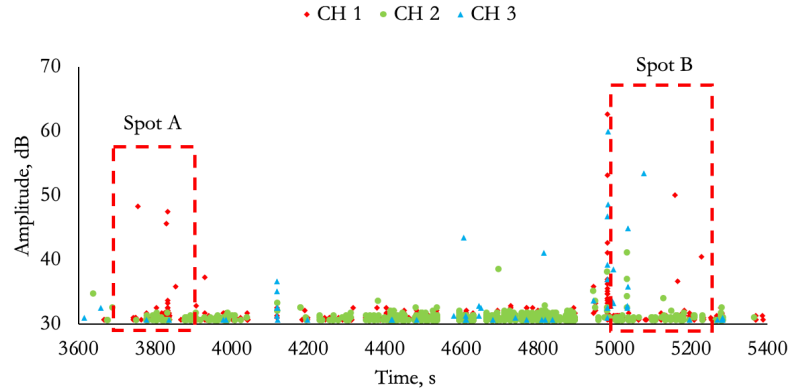

FIGURE 9. Amplitude against time at different channel for asphalt pavement (3rd Interval)

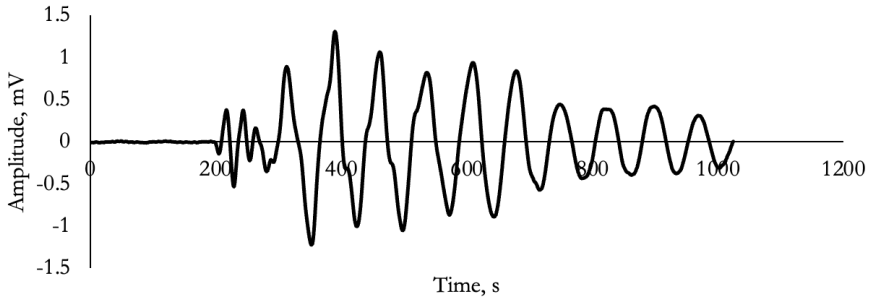

FIGURE 10. Maximum signal for peak amplitude at 3rd interval

The analysis of AE amplitude indicates that the vehicle class has a significant impact on sound emissions. This is because the vehicle class influences the load applied to the asphalt pavement at a given time. Based on this monitoring, it is evident that vehicle loading can contribute to higher recorded amplitudes. According to Ma and Du (2020), high amplitudes are associated with heavy loads, but low loads can also result in high amplitudes due to the presence of noise signals. Small loads correspond to low average amplitudes, while large load forces typically lead to higher maximum amplitudes. Signals with large amplitudes serve as a warning sign for potential microcrack formation. Jiao et al. (2019) also observed an increase in sound emission amplitude with increasing load. Md Nor et al. (2021) confirm that cyclic loading impacts AE activities.

RISE TIME

Figure 11-13 depicts the variance of rise time values from three different channels at three different intervals. The rise time performance of all three channels significantly differs in the 1st interval. CH 1 recorded the highest rise time value, while CH 3 recorded the lowest. CH 2 captured a wider range of data compared to the other two channels; however, CH 3 only recorded a few rise time readings. A similar performance gap across the three channels is observed in the 2nd interval.

However, CH 2 recorded more values than CH 1 and CH 3. CH 2 also recorded the highest and lowest rise time values, which were 686.8 µs and 2.2 µs, respectively. For example, in the 1st interval, CH 2 exhibits a wider range

of rise time values. Unlike in the 1st interval, CH 1 recorded the lowest rise time readings in the 2nd interval. Finally, the three channels display different behaviours in the 3rd interval, similar to the 1st interval. Unlike the 1st and 2nd intervals, the three channels in the 3rd interval showed a greater variety of rise time values. In the 3rd interval, CH 1 recorded the highest rise time readings, while CH 3 recorded the least. The maximum rise time values of asphalt pavement from the three different channels are presented in Table 4. The 1st interval of CH 1 has the highest rise time value among the three channels, measuring 2616 µs, while CH 3 has the lowest value. The rise time values across the three channels display different patterns, attributable to variations in the traffic load experienced during monitoring. In CH 1, the value decreases from the 1st to the 3rd interval. CH 3's rise time values are the opposite of CH 1, while CH2's rise time value increases from the 1st to the 2nd interval and decreases from the 2nd to the 3rd interval corresponding to an increase in traffic load during the 2nd interval. According to Jiao et al. (2018), a low and discontinuous rise time value is associated with crack initiation. Shahidan et al. (2013) also stated that AE waveforms frequently indicate a tensile crack with a shorter rise time and a high average frequency. The results obtained in this study suggest the possibility of micro-crack initiation during the monitoring. Furthermore, it can be observed that the 1st interval recorded the lowest rise time readings in the three channels. This is because the 1st interval recorded the lowest total number of vehicles passing by, hence the lowest cyclic loading from vehicles.

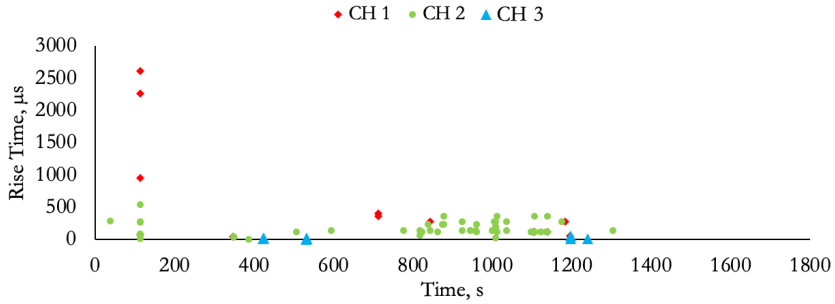

FIGURE 11. Rise time against at different channel fo asphalt pavement (1st Interval)

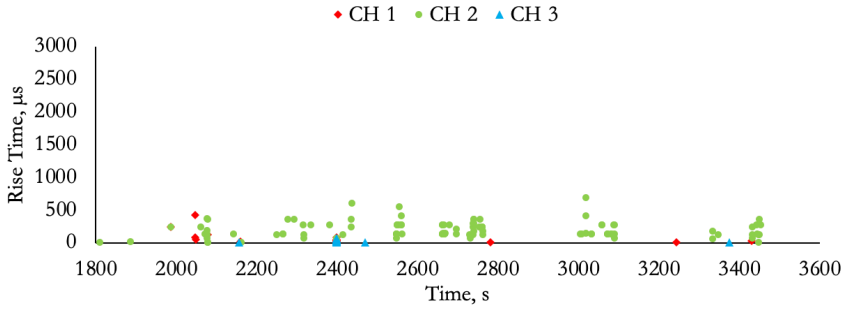

FIGURE 12. Rise time against time at different channel for asphalt pavement (2nd Interval)

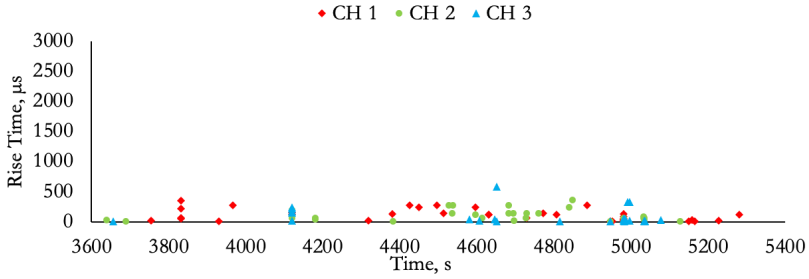

FIGURE 13. Rise time against time at different channel for asphalt pavement (2nd Interval)

TABLE 4. Maximum recorded rise time over different channels for three intervals

	Maximum Recorded Rise Time, μs		
Channel	1st Interval	2nd Interval	3rd Interval
CH 1	2616.0	423.6	349.6
CH 2	545.6	686.8	360.0
CH 3	59.8	73.2	582.4

RISE ANGLE

The variations in rise angle values from three different channels at three intervals are shown in Figure 14-16. During the 1st interval, the rise angle performance of all three channels is dissimilar. However, CH 2 exhibits higher rise angle values than the other two channels. The range of rise angle values between the three channels differs significantly. The highest rise angle value is recorded on CH 1, while the lowest is recorded on CH 3. In the 2nd interval, there is also a disparity in performance between the three channels, with CH 2 displaying higher rise angle readings. CH 2 has a wider variety of rise angle values. The maximum rise angle is recorded on CH 2, and the lowest on CH 3. Finally, like the 1st and 2nd intervals, the three channels behave differently in the 3rd interval. However, all three channels exhibit a wider range of rise angle values. Furthermore, CH 3 does not record as many rise angle readings as the other two channels. Table 5 displays the maximum AE rise angle values of the asphalt pavement from the three distinct channels. CH 1 has the highest rise angle of the three channels, measuring 39.8 s/V in the 1st interval. The highest rise angle value recorded in the 2nd and 3rd intervals is from CH 2. The AE rise angle values measured in the three channels follow a varied pattern, which correlates with variation in the loading type of each vehicle. The value decreases from the 1st to the 2nd interval and then increases from the 2nd to the 3rd interval in CH 1. The rise angle values recorded by CH 2 are reversed from CH 1, while the value from CH 3 decreases from the 1st to the 3rd interval. Rise angle is the ratio of rise time to amplitude. The values of rise angle in the three intervals are highly influenced by the rise time values. This can be observed in the distribution pattern of rise angle and rise time values in Figures 11-13 and 14-16, respectively. The high values of rise angle in the 1st interval, at 113s recorded by CH 1, are influenced by the high values of rise time. Rise angle serves as an indicator of shear crack propagation. A study by Md Nor et al. (2021) indicated that the rise angle values obtained were due to the formation of shear cracks. The low values of the rise angle recorded could indicate the potential for shear crack initiation in the asphalt pavement layers. A study by Jiao et al. (2019) found that the presence of rise angle with low values was considered as micro-crack nucleation, while rise angle values reaching their maximum indicate rapid growth of shear cracks until specimen failure. Concerning this study, it is expected that the formation of micro-cracks in the asphalt pavement is due to cyclic loading from vehicles passing by.

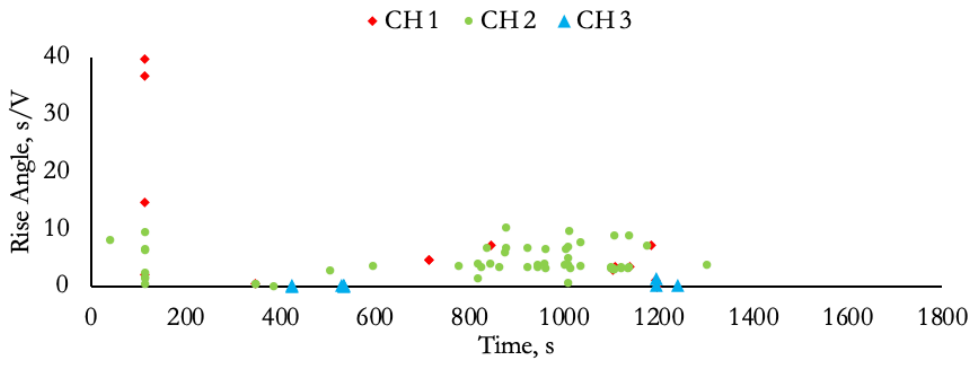

FIGURE 14. Rise angle against time at different channels for asphalt pavement (1st Interval)

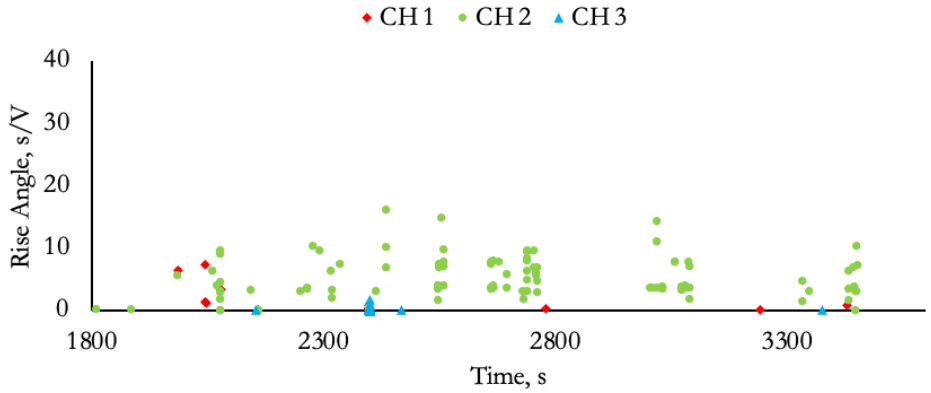

FIGURE 15. Rise angle against time at different channel for asphalt pavement (2nd interval)

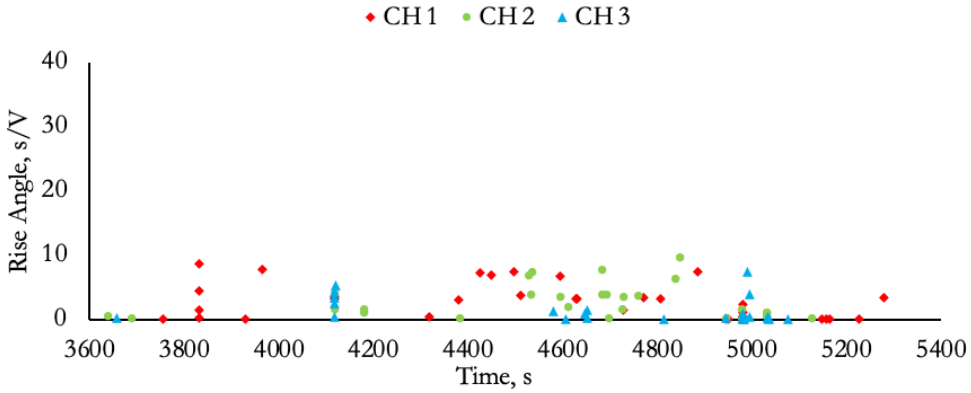

FIGURE 16. Rise angle against time at different channel for asphalt pavement (3rd Interval)

TABLE 5. Rise angle against time at different channel for asphalt pavement (3rd Interval)

	Maximum Recorded Rise Angle, s/V		
Channel	1st Interval	2nd Interval	3rd Interval
CH 1	39.8	7.4	8.7
CH 2	10.3	16.2	9.7
CH 3	1.2	1.7	7.5

AVERAGE FREQUENCY

The variation in average frequency values from three different channels at three intervals is shown in Figure 17-19. It is evident that the average frequency performance of all three channels differs in the 1st interval. CH 2 recorded more values from 800 s to 1200 s, with the highest average frequency value among all channels, while CH 1 recorded the lowest value. In the 2nd interval, the variance of values between the three channels also differs. Similar to the 1st interval, CH 2 recorded the highest value. Additionally, CH 3 recorded a repetitive value at 2398 s. Finally, in the 3rd interval, the three channels exhibit different behaviour. CH 1 recorded more varied values than the other two channels, and it recorded the highest average frequency values at 4946 s and 5149 s.

Table 6 displays the maximum average frequency values obtained during the monitoring work. It can be observed that these values are relatively small compared to the other parameters. CH 2 recorded the highest average frequency value across the three intervals due to the highest numbers of vehicle recorded during monitoring, while CH 3 recorded the lowest. The pattern of maximum values for each channel varies due to different loads related with the various types of vehicles that passed through the road. In the 1st interval, the value increases from the 1st to the 3rd interval. In the 2nd interval, the value increases from the 1st to the 2nd interval but decreases from the 2nd to the 3rd interval. Finally, in the 3rd interval, the values recorded contrast the 2nd interval. Average frequency is often associated with tensile cracks. Jiao et al. (2019) found that the average frequency values obtained were few and small

and correlated with the nucleation of tensile cracks. Xu et al. (2021) also emphasised the importance of the distribution of average frequency distribution in determining the shift in fracture modes from shear to tensile failure. The distribution of average frequency values obtained by Xu et al. (2021) revealed that the test specimens exhibited tensile failure. However, the values obtained in this study are relatively small, suggesting the possibility of only micro-crack initiations.

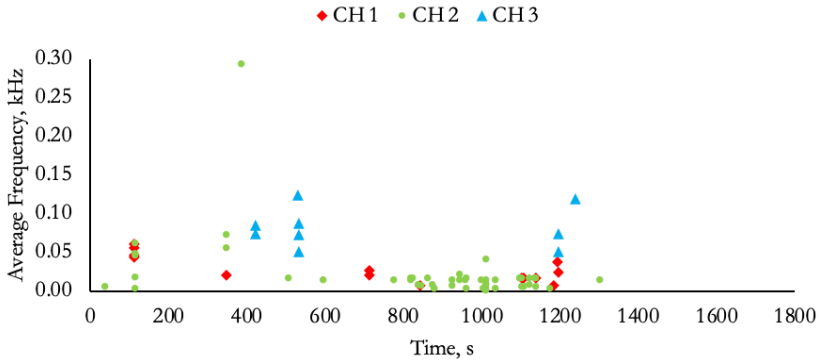

FIGURE 17. Average frequency against time at different channels for asphalt pavement (1st Interval)

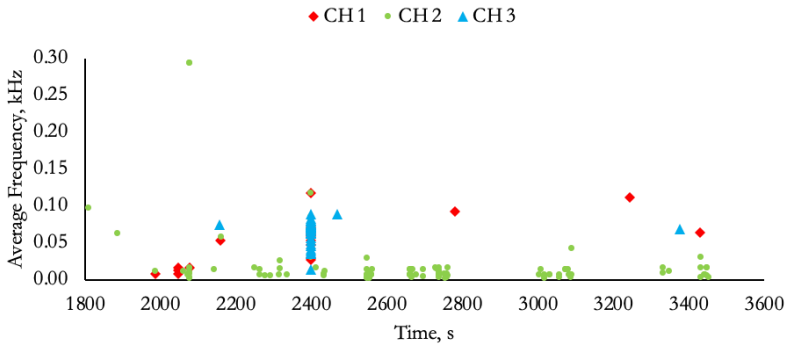

FIGURE 18. Average frequency against time at different channels for asphalt pavement (2nd Interval)

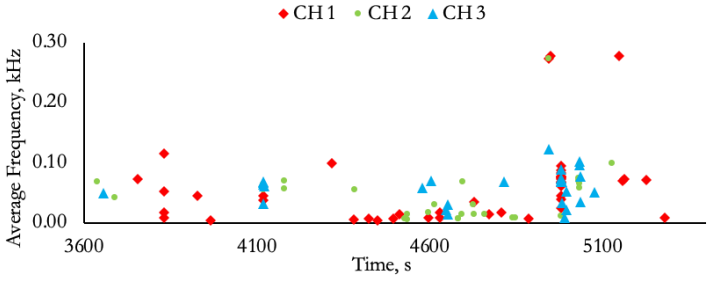

FIGURE 19. Average frequency against time at different channels for asphalt pavement (3rd Interval)

TABLE 6. Maximum recorded average frequency over different channels for three intervals

	Maximum Recorded Average Frequency, kHz		
Channel	1st Interval	2nd Interval	3rd Interval
CH 1	0.06	0.11	0.28
CH 2	0.29	0.45	0.27
CH 3	0.13	0.08	0.10

RELATIONSHIP BETWEEN AVERAGE FREQUENCY AND RISE ANGLE VALUE

Figure 20-22 illustrates the variance of average frequency versus rise angle values from three channels at three different intervals. Each interval displays a distinct distribution of values for the three channels. Observing the 2nd interval, it is evident that the three channels recorded higher values, followed by the 3rd and 1st intervals. This outcome may be influenced by cyclic loading from vehicles. The reason is that the 2nd interval documented the highest number of passing vehicles, while the 1st interval recorded the lowest. The highest average frequency value is recorded in CH 2 during the second interval, while the highest rise angle value is recorded in CH 1 during the first interval. The pattern of average frequency values in CH 1 differs from CH 2 and CH 3.

The average frequency values in CH 1 increase from the 2nd to the 3rd interval, while CH 2 and CH 3 increase from the 1st interval to the 2nd interval and decrease from the 2nd to the 3rd interval. The pattern of rise angle values can only be seen in CH 1. The rise angle values in CH 2 and CH 3 remain constant throughout the three intervals. The rise angle values in CH 1 decrease from the first to the 3rd interval. Additionally, in the 1st interval, it can be observed that values from CH 1 and CH 2 tend towards the horizontal axis, while values from CH 3 tend towards the vertical axis. In contrast to the 1st interval, values recorded by CH 1 tend towards the vertical axis during the 2nd interval. However, values from CH 2 and CH 3 exhibit the same behaviour as in the 1st interval. Unlike the 1st and 2nd intervals, the values from the three channels show a more balanced distribution towards both axes. From a broader perspective, the average frequency and rise angle distribution for all three intervals tend towards both axes.

Basically, the correlation between average frequency and rise angle is associated with shear and tensile cracks. Li et al. (2023) indicated that when the average frequency value is large and the rise angle value is small, the structure is considered to have tensile crack. When the rise angle value is large and the average frequency value is small, the structure is considered to have shear crack. Zhu et al. (2020) further stated that the properties of rise angle and average frequency are crucial in characterizing tensile and shear modes. Tensile wave modes exhibit a shorter rise and duration time, higher amplitude, and higher counts, resulting in a higher average frequency and lower rise angle. In contrast, shear wave modes have a longer rise time and duration time, leading to a higher rise angle and lower average frequency values. Average frequency and rise angle values are relatively low across three channels at three different intervals in this study. Consequently, the results may indicate a potential tendency for the initiation of shear and tensile microcracks in the pavement structure.

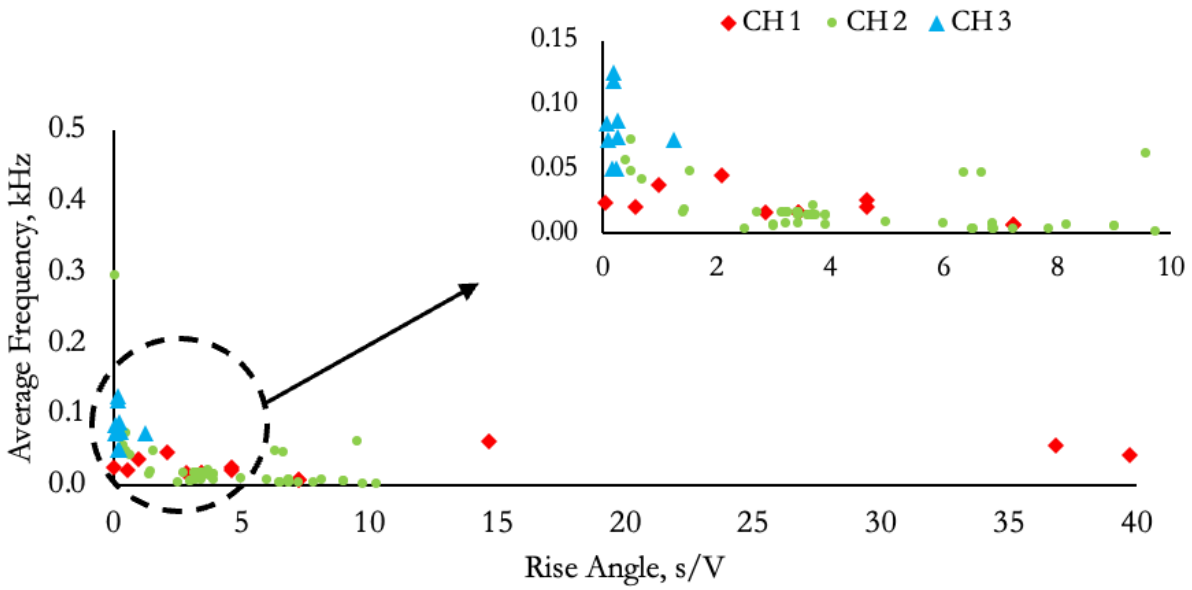

FIGURE 20. Average frequency against rise angle at different channel for asphalt pavement (1st Interval)

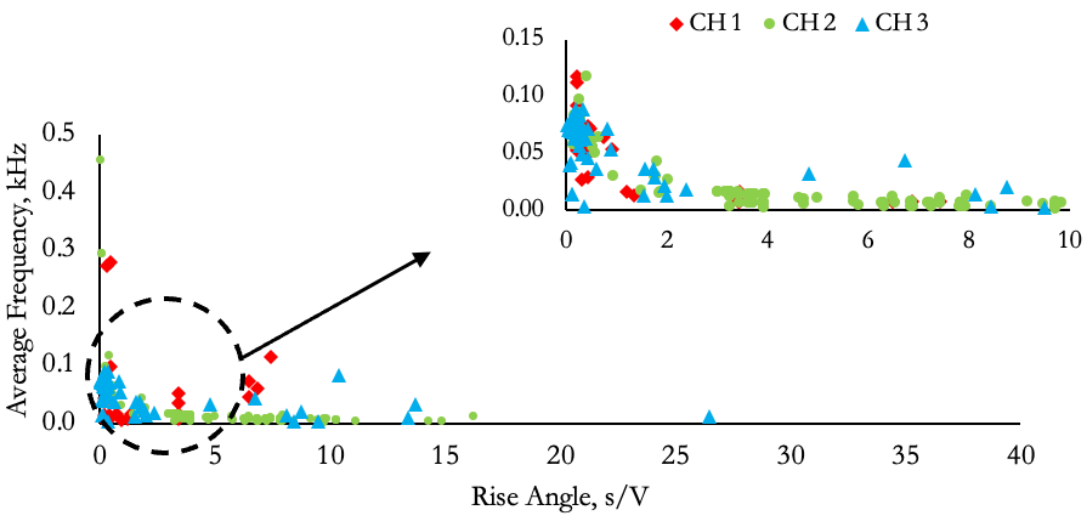

FIGURE 21. Average frequency against rise angle at different channel for asphalt pavement (2nd interval)

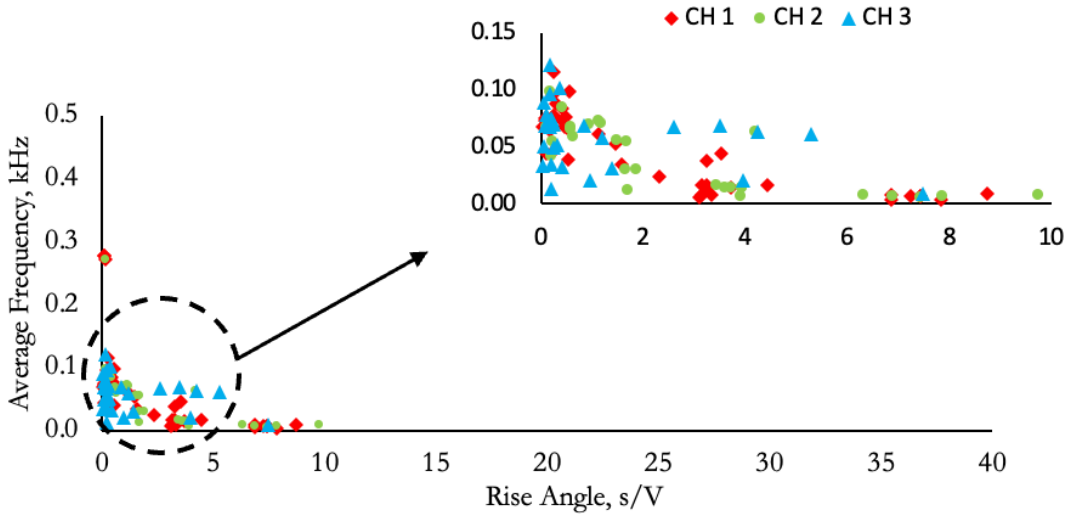

FIGURE 22. Average frequency against rise angle at different channel for asphalt pavement (3rd Interval)

CONCLUSION

This study evaluated the ability of the AE technique for real-time monitoring of asphalt pavement structures. Two main conclusions can be drawn from this study. First, the distribution of parameter values varies among the three different channels over the three intervals. The results suggest that the distribution and behaviour of these parameters are influenced by cyclic loading caused by passing vehicles. The parameter values of AE, amplitude, rise time, and average frequency, increase with the increasing cyclic load from moving vehicles. Previous studies have associated the variation of these parameters with the nucleation and initiation of cracks. However, the values obtained in this study are relatively small, indicating the potential initiation of only micro-cracks in the asphalt pavement layers.

Secondly, a strong correlation between average frequency and rise angle values was observed, which is highly associated with tensile and shear cracks. This correlation has been supported by numerous previous studies. However, in this study, the correlation between these two parameters is associated with the potential initiation of tensile and shear microcracks. This is because both the average frequency and rise angle values are remarkably small. Furthermore, the average frequency and

rise angle values obtained in this study are influenced by the number of passing vehicles. The higher number of vehicles results in higher loads and, consequently, higher recorded values. The findings of this study will contribute to the development of a reliable and efficient field monitoring method for asphalt pavements.

ACKNOWLEDGEMENT

This research has received no external funding.

DECLARATION OF COMPETING INTEREST

None.

REFERENCES

Apeagyei, A. K. 2013. Evaluating foamed asphalt stability using acoustic emission techniques. *Journal of Materials in Civil Engineering* 25(9): 1291–1298.

Apeagyei, A. K., Buttlar, W. G., and Reis, H. 2009. Assessment of low-temperature embrittlement of asphalt binders using an acoustic emission approach. *Insight: Non-Destructive Testing and Condition Monitoring* 51(3): 129–136.

Arnold, J. W., Behnia, B., McGovern, M. E., Hill, B., Buttlar, W. G., and Reis, H. 2014. Quantitative evaluation of low-temperature performance of sustainable asphalt pavements containing recycled asphalt shingles (RAS). *Construction and Building Materials* 58: 1–8.

ASTM E 2374: 2010. *Standard Guide for Acoustic Emission System Performance Verification*. ASTM Int.

ASTM E976-15: 2015. *Standard Guide for Determining the Reproducibility of Acoustic Emission Sensor Response*. ASTM Int.

Behnia, B., Buttlar, W., and Reis, H. 2018. Evaluation of low-temperature cracking performance of asphalt pavements using Acoustic Emission: A review. *Applied Sciences* (Switzerland): 8(2): 1–20.

Behnia, B., Dave, E. v., Buttlar, W. G., and Reis, H. 2016. Characterization of embrittlement temperature of asphalt materials through implementation of acoustic emission technique. *Construction and Building Materials* 111: 147–152.

Cong, L., Zhang, Y., Xiao, F., and Wei, Q. 2016. Laboratory and field investigations of permeability and surface temperature of asphalt pavement by infrared thermal method. *Construction and Building Materials* 113: 442–448.

Hashim, K.A., Nor, N.M., Abdullah, S., Aziz, F.F., and Idrus, J. 2021. Determination of acoustic emissions data characteristics under the response of pencil lead fracture procedure. *J Fail. Anal. and Preven*. 21: 2064–2071.

Hill, B., Behnia, B., Buttlar, W. G., and Reis, H. 2013. Evaluation of warm mix asphalt mixtures containing reclaimed asphalt pavement through mechanical performance tests and an acoustic emission approach. *Journal of Materials in Civil Engineering* 25(12): 1887–1897.

Ji, X., Hou, Y., Chen, Y., and Zhen, Y. 2019. Attenuation of acoustic wave excited by piezoelectric aggregate in asphalt pavement and its application to monitor concealed cracks. *Construction and Building Materials* 216: 58–67.

Jiao, Y., Zhang, Y., Zhang, M., Fu, L., and Zhang, L. 2019. Investigation of fracture modes in pervious asphalt under splitting and compression based on acoustic emission monitoring. *Engineering Fracture Mechanics* 211: 209–220.

Li, J., Wang, L., Zhang, X., Miao, Y., Guo, Y., and Wang, Y. 2023. Cracking process analysis and fracture pattern recognition of asphalt mixture based on acoustic emission characteristics. *Journal of Materials in Civil Engineering* 35(12).

Li, X., and Marasteanu, M. O. 2006. Investigation of low temperature cracking in asphalt mixtures by acoustic emission. *Road Materials and Pavement Design* 7(4): 491–512.

Ma, G., and Du, Q. 2020. Structural health evaluation of the prestressed concrete using advanced acoustic emission (AE) parameters. *Construction and Building Materials* 250.

Md Nor, N., Abdullah, S., and Mat Saliah, S.N. 2021. On the need to determine the acoustic emission trend for reinforced concrete beam fatigue damage, *International Journal of Fatigue* 152.

Md Nor, N., Muhamad Bunnori, N., Ibrahim, A., and Mohd Saman, H. 2013. Acoustic emission signal for fatigue crack classification on reinforced concrete beam. *Construction and Building Materials* 49: 583–590.

Noorsuhada M.N. 2016. An overview on fatigue damage assessment of reinforced concrete structures with the aid of acoustic emission technique. *Construction and Building Materials* 112: 424–439.

Qiu, J., Yang, Q., Qiu, X., Xiao, S., He, L., and Hu, G. 2022. Use of acoustic emission for exploring characteristics and behaviors of mixed-mode fracture process of asphalt mixtures. *Materials and Structures* 55(7).

Qiu, X., Wang, Y., Xu, J., Xiao, S., and Li, C. 2020. Acoustic emission propagation characteristics and damage source localization of asphalt mixtures. *Construction and Building Materials* 252: 119086.

Seo, Y., and Kim, Y. R. 2008. Using acoustic emission to monitor fatigue damage and healing in Asphalt Concrete. *KSCE Journal of Civil Engineering* 12(4): 237–243.

Shahidan, S., Pulin, R., Muhamad Bunnori, N., and Holford, K. M. 2013. Damage classification in reinforced concrete beam by acoustic emission signal analysis. *Construction and Building Materials* 45: 78–86.

Shen, G., Qiu, X., Tao, J. Q., Du, N. D., and Hu, Y. J. 2015. Diagnostic testing on crack propagation of Asphalt Pavement Materials. *Key Engineering Materials* 667: 396–401.

Wei, H., Zhang, H., Li, J., Zheng, J., and Ren, J. 2023. Effect of loading rate on failure characteristics of asphalt mixtures using acoustic emission technique. *Construction and Building Materials* 364: 129835.

Xu, J., Ashraf, S., khan, S., Chen, X., Akbar, A., and Farooq, F. 2021. Micro-cracking pattern recognition of hybrid CNTs/GNPs cement pastes under three-point bending loading using acoustic emission technique. *Journal of Building Engineering* 42.

Zhu, B., Liu, H., Li, W., Wu, C., and Chai, C. 2020. Fracture behavior of permeable asphalt mixtures with steel slag under low temperature based on acoustic emission technique. *Sensors* (Switzerland) 20(18): 1–24.

Zhu, C., Cheng, P., and Zhao, G. 2020. Study on the main characteristics of reflective cracking in the asphalt overlay on an old cement pavement. *Materials Science Forum* 980: 244–253.